

**Table I. Comparison of measured and calculated (Eq. 5) diffusion coefficients.**

Temperature (°C)	$D_{\text{eff}}$ (cm <sup>2</sup> /s)	
	Measured <sup>a</sup>	Calculated <sup>b</sup>
400	1.95 to $4.0 \times 10^{-10}$	$1.75$ to $3.75 \times 10^{-10}$ (7 to 13D)
450	$4.3$ to $8.1 \times 10^{-10}$	$6.0$ to $10.8 \times 10^{-10}$ (5 to 9D)
500	$1.55$ to $2.9 \times 10^{-9}$	$1.35$ to $2.25 \times 10^{-9}$ (3 to 5D)

<sup>a</sup> Range calculated from data in Fig. 3.

<sup>b</sup> Using  $D$  from Fig. 4.

$$D_{\text{eff}} = D \left( 1 + \frac{2k}{d} \right) \quad [5]$$

where  $k$  ranged from 0.015 at 400°C to 0.005 at 500°C. A comparison of the measured coefficients with calculated values of  $D_{\text{eff}}$  from Eq. 5 using  $d = 25$  to  $50 \mu\text{m}$  (Table I) shows good agreement given the uncertainty and variability in the grain size.

Also, the apparent activation energy for  $D_{\text{eff}}$  (~85 kJ/mol) agrees closely with the 92.5 kJ/mol value found for grain boundary etch marker movement.<sup>13</sup>

Manuscript submitted Nov. 18, 1996; revised manuscript received Dec. 19, 1996.

Kaiser Aluminum & Chemical Corporation assisted in meeting the publication costs of this article.

#### REFERENCES

1. F. Keller and R. H. Brown, *Met. Technol. (AIME)*, Publ. No. 1659, p. 1 (1944).
2. J. Crank, *The Mathematics of Diffusion*, p. 15, Clarendon Press, Oxford (1975).
3. W. W. Binger, E. H. Hollingsworth, and D. O. Sprowls, in *Aluminum: Properties, Physical Metallurgy, and Phase Diagrams*, p. 210, ASM, Metals Park, OH (1967).
4. H. W. L. Phillips, *Equilibrium Diagrams of Aluminum Alloy Systems*, p. 58, The Aluminum Development Assoc., London (1961).
5. M. S. Anand, S. P. Murarka, and R. P. Agarwala, *J. Appl. Phys.*, **36**, 3860 (1965).
6. Y. Minamino, Y. Yamane, and T. Takahashi, *J. Mater. Sci. Lett.*, **4**, 797 (1985).
7. D. McLean, *Grain Boundaries in Metals*, p. 225, Oxford Press, Oxford (1957).
8. J. C. Fisher, *J. Appl. Phys.*, **22**, 74 (1951).
9. R. T. Whipple, *Philos. Mag.*, **45**, 1225 (1954).
10. H. S. Levine and C. J. MacCallum, *J. Appl. Phys.*, **31**, 595 (1960).
11. A. D. LeClaire, in *Solute-Defect Interactions: Theory and Experiment*, p. 251, Pergamon Press, Elmsford, NY (1986).
12. E. W. Hart, *Acta Metall.*, **5**, 597 (1957).
13. R. C. Dorward, *Met. Mater. Trans.*, In press.

## Reduced-Temperature Solid Oxide Fuel Cell Based on YSZ Thin-Film Electrolyte

Selmar de Souza, Steven J. Visco,\* and Lutgard C. De Jonghe

Materials Science Division, Lawrence Berkeley National Laboratory, University of California, Berkeley, California 94720, USA

#### ABSTRACT

A planar thin-film solid oxide fuel cell has been fabricated with an inexpensive, scalable, technique involving colloidal deposition of yttria-stabilized zirconia (YSZ) films on porous NiO-YSZ substrates, yielding solid oxide fuel cells capable of exceptional power density at operating temperatures of 700 to 800°C. The thickness of the YSZ film deposited onto the porous substrate is approximately 10  $\mu\text{m}$  after sintering, and is well bonded to the NiO/YSZ substrate. Ni-YSZ/YSZ/LSM cells built with this technique have exhibited theoretical open-circuit potentials (OCVs), high current densities, and exceptionally good power densities of over 1900 mW/cm<sup>2</sup> at 800°C. Electrochemical characterization of the cells indicates negligible losses across the Ni-YSZ/YSZ interface and minor polarization of the fuel electrode. Thin-film cells have been tested for long periods of time (over 700 h) and have been thermally cycled from 650 to 800°C while demonstrating excellent stability over time.

#### Introduction

The high operating temperatures (~1000°C) of solid oxide fuel cells (SOFCs) can lead to complex materials problems which include electrode sintering, interfacial diffusion between electrolyte and electrode materials, and mechanical stress due to different thermal expansion coefficients of the cell components. Such problems have limited the commercial development of SOFCs. Accordingly, it may be desirable to operate SOFCs at reduced temperatures (within the practical range for methane reforming), assuming this can be done without sacrificing performance. Lower operating temperatures allow a wider choice of materials to be used as interconnects, including metal alloys. Approaches to minimize resistive losses across the electrolyte have included replacing YSZ by alternative electrolyte materials with higher ionic conductivity, and/or reducing the thickness of the solid oxide electrolyte from that in conventional cells (100 to 200  $\mu\text{m}$ ) to approximately 10  $\mu\text{m}$ .

Several methods for depositing thin films onto porous substrates (CVD/EVD, sputtering, sol-gel deposition among others) have been reported.<sup>1-5</sup> In this paper we describe an inexpensive approach for thin-film deposition using colloidal techniques, and the exceptional performance attained for SOFCs fabricated with this procedure.

#### Experimental

Yttria-stabilized zirconia (YSZ) powder from Tosoh Corporation and nickel oxide (NiO) powder from J. T. Baker was mixed approximately as 50/50 weight percent (w/o), respectively. The anode powders were then compacted under uniaxial pressure. Green NiO-YSZ anode disks were subsequently fired at 950°C for 4 h to coarsen the microstructure. YSZ powders mixed in isopropanol were sonicated with a high intensity ultrasonic probe to form a stable colloidal dispersion of submicron polycrystalline electrolyte powders. To avoid cracking of the YSZ thin film due to stress built up by the 2D confinement of the film during sintering, the shrinkage of the substrate was carefully matched to the shrinkage profile of the YSZ thin film. In this way, the film is under compression rather than tension while sintering.<sup>6</sup> The YSZ electrolyte film was applied with a single casting step, and the electrolyte/electrode bilayer was then fired at 1400°C for 4 h to achieve a fully densified YSZ film.

$\text{La}_{0.85}\text{Sr}_{0.15}\text{MnO}_3$  (LSM) powders were prepared by the glycine-nitrate process as described in Ref. 7. LSM was mixed with YSZ in a ratio 50/50 w/o. The LSM/YSZ powder was then mixed with ethylene glycol to form a paste, applied onto an NiO-YSZ/YSZ bilayer, and sintered at 1250°C for ~1 h. The LSM air electrodes were ~100  $\mu\text{m}$  in thickness after sintering.

Platinum mesh was used as the current collector for both the LSM air electrode and the Ni-cermet fuel electrode. Two wires were spot-welded to each current collector so that fuel cell potentials could be measured at the noncurrent carrying leads.

\* Electrochemical Society Active Member.

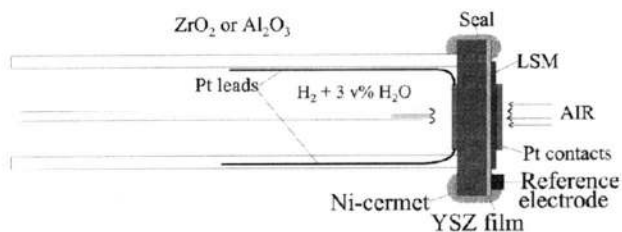


Fig. 1. Fuel cell testing assembly diagram.

Ceramic adhesives were used to fix and seal the fuel cell/current collector structure to an alumina or zirconia tube which was used as a fuel cell testing assembly (Fig. 1). Hydrogen saturated with H<sub>2</sub>O at room temperature was used as fuel. Air was used as oxidant and was supplied to the cathode by ambient flow. Since the H<sub>2</sub>/H<sub>2</sub>O stream was not preheated, there was some cooling of the fuel cell relative to the furnace temperature. A platinum reference electrode was bonded onto the thin electrolyte film, at several millimeters from the working electrode on the air side. Current interrupt and/or impedance spectroscopy was used to measure the ohmic resistance of the fuel cell.

Results and Discussion

The performance of SOFCs, H<sub>2</sub> + 3 volume percent (v/o) H<sub>2</sub>O, Ni-YSZ/YSZ/La<sub>0.85</sub>Sr<sub>0.15</sub>MnO<sub>3</sub>, air, were evaluated under current control. Figure 2 shows current-voltage (*I*-*V*) curves for a single cell tested at 800°C. The maximum power density achieved was 1935 mW/cm<sup>2</sup> at a current density of 4.5 A/cm<sup>2</sup> and cell voltage of 0.43 V (LBNL cells typically exceed 1.8 W/cm<sup>2</sup> at 800°C). This result illustrates the exceptional performance achievable for YSZ thin-film electrolyte-based SOFCs operating at reduced temperatures. Cells of this type have been operated at power densities of 800 mW/cm<sup>2</sup> for more than 700 h with no detectable loss in performance.

Figure 3 shows the voltage drop vs. current for a thin-film cell. The total voltage drop was separated into ohmic and nonohmic contributions by the current interrupt method. The use of a reference electrode allowed separation of anodic and cathodic contributions to cell polarization. The YSZ *IR* drop is estimated from the known conductivity and thickness of the electrolyte (10 μm). As can be seen from Fig. 3, even at very high current densities, the voltage drop due to a 10 μm YSZ electrolyte film is almost negligible. The remainder of the ohmic drop is probably due to contact resistance at the LSM/YSZ interface as well as minor losses across the current collectors. The ohmic loss across the Ni-YSZ/YSZ interface is essentially negligible. The polarization of the electrodes ( $\eta_a + \eta_c$ ) account for about 40% of the total voltage drop. The cathodic polarization ( $\eta_c$ ) was larger than the anodic polarization ( $\eta_a$ ) which was almost negligible ( $\eta_a$ ) for current densities below 2.0 A/cm<sup>2</sup>. The YSZ electrolyte *IR* drop represents about 18% of the total voltage drop.

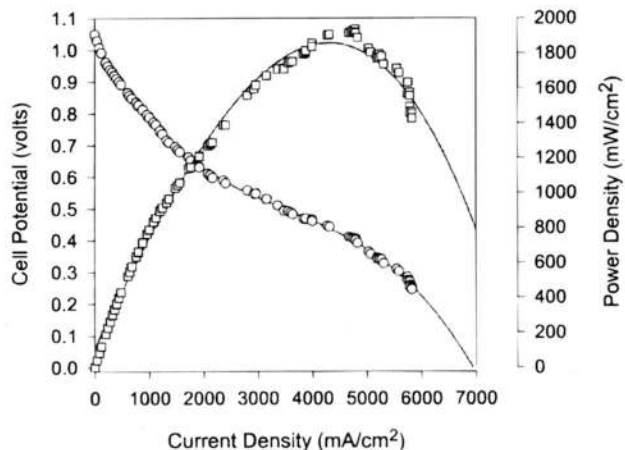


Fig. 2. *I*-*V* characteristics of a (H<sub>2</sub> + v/o H<sub>2</sub>O), Ni-YSZ/YSZ/LSM, (air) fuel cell at 800°C.

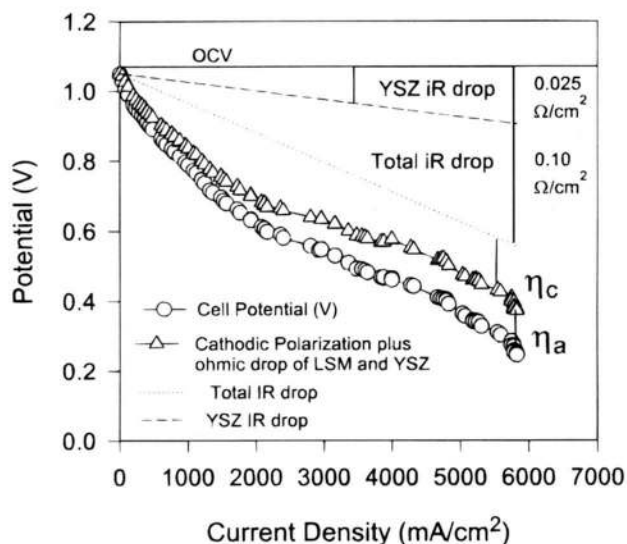


Fig. 3. Separation of cell polarization components by current interrupt techniques; total resistance calculated from the ohmic drop (*IR*) of the cell;  $\eta_c$ , cathode polarization;  $\eta_a$ , anode polarization, and the YSZ electrolyte *IR* drop.

Figures 4 and 5 show the cross sections of the Ni-cermet/YSZ/Pt and Ni-YSZ/YSZ/LSM fuel cell structures, which have been reduced in hydrogen at 800°C. It is observed that the thin-YSZ electrolyte film is uniformly continuous, pore free, and well adhered to the porous Ni-YSZ fuel electrode. The Ni-cermet is highly uniform with an even distribution of pores and good particle to particle contact. The LSM electrode (Fig. 5) appears to have a less uniform structure when compared to the Ni-cermet which may account for the larger cathodic polarization relative to anodic polarization over most of the *I*-*V* curve.

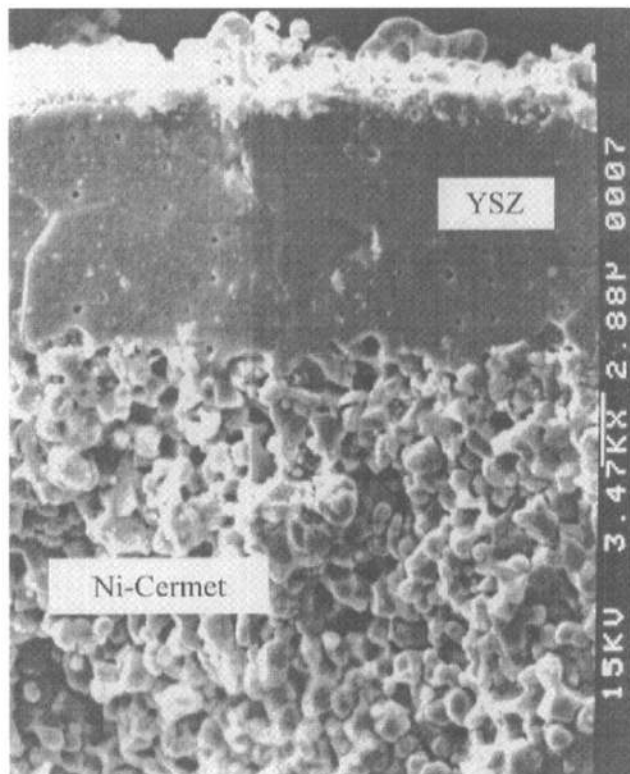


Fig. 4. Scanning electron micrograph of a Ni-cermet/YSZ/Pt thin-film fuel cell cross section. YSZ electrolyte film is 9 μm thick. NiO-YSZ was reduced *in situ* with H<sub>2</sub>/H<sub>2</sub>O at 800°C to yield final Ni-YSZ cermet structure.

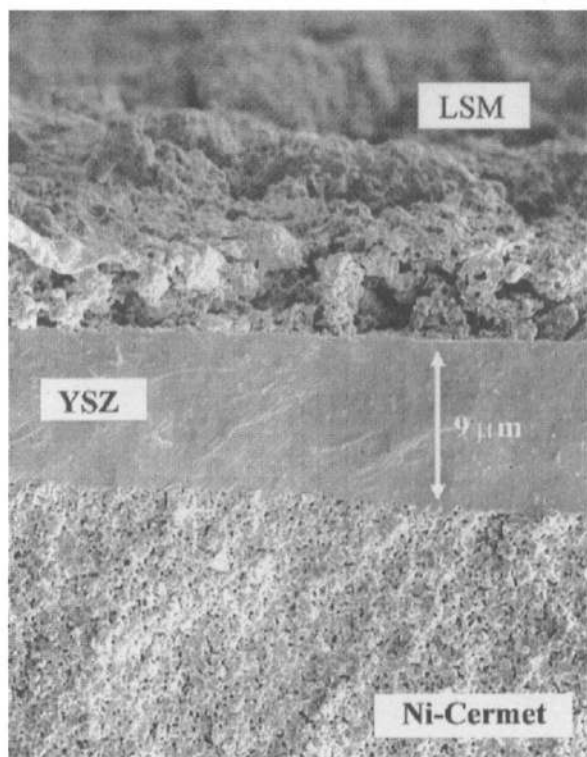


Fig. 5. SEM micrograph showing cross section of a Ni-Cermet/YSZ/LSM thin-film fuel cell that was thermally cycled and tested over 400 h.

### Conclusions

A highly successful procedure has been developed which allows deposition of thin-film ceramics on highly porous substrates. The

methodology is inexpensive and scalable. Thin-film SOFCs fabricated using these techniques demonstrate performances of close to  $2 \text{ W/cm}^2$  at  $800^\circ\text{C}$ . Current interrupt techniques indicate the majority of the voltage loss at high current density is due to ohmic losses, most likely associated with cathode/electrolyte contact resistance ( $0.1 \Omega \text{ cm}^2$ ). The exceptional performance of the thin-film SOFCs implies that reduced temperature operation is possible while still maintaining high power density.

### Acknowledgment

This research was supported by the Laboratory Technology Research Program (ER-LTR), Office of Computational and Technology Research, U.S. Department of Energy under a CRADA (Cooperative Research and Development Agreement) between Ernest Orlando Lawrence Berkeley National Laboratory (Berkeley Lab) and The Electric Power Research Institute (EPRI), Palo Alto, CA 94303, under U.S. DOE Contract DE-AC03-76SF00098.

Manuscript submitted Sept. 23, 1996; revised manuscript received Oct. 20, 1996.

Lawrence Berkeley National Laboratory assisted in meeting the publication costs of this article.

### REFERENCES

1. N. W. Minh, *J. Am. Ceram. Soc.*, **76**, 563 (1993).
2. A. Negishi, K. Nozaki, and T. Ozawa, *Solid State Ionics*, **3/4**, 443 (1981).
3. A. O. Isenberg, *ibid.*, **3/4**, 431 (1981).
4. T. Setogushi, T. Inou, H. Takebe, K. Eguchi, K. Morinaga, and H. Arai, *This Journal*, **139**, 2875 (1992).
5. U. B. Pal and S. C. Singhal, *ibid.*, **137**, 2937 (1990).
6. S. J. Visco, L.-S. Wang, S. Souza, L. C. De Jonghe, *Mater. Res. Soc. Symp. Proc.*, **369**, 683 (1995).
7. L. A. Chick, L. R. Pederson, G. D. Maupin, J. L. Bates, L. E. Thomas, and G. I. Exartos, *Mater. Lett.*, **10**, 6 (1990).

## Highly Selective Chemical Etching of Si vs. $\text{Si}_{1-x}\text{Ge}_x$ Using $\text{NH}_4\text{OH}$ Solution

Feng Wang,\* Yi Shi, Jianlin Liu, Yang Lu, Sulin Gu, and Youdou Zheng

Department of Physics and Institute of Solid State Physics, Nanjing University, Nanjing 210093, China

### ABSTRACT

Highly selective chemical etching of Si vs. epitaxial  $\text{Si}_{1-x}\text{Ge}_x$  in  $\text{NH}_4\text{OH}$  solution has been investigated. It was found the selectivity was better than 80:1 even for a  $\text{Si}_{0.9}\text{Ge}_{0.1}$  in 10 weight percent (w/o)  $\text{NH}_4\text{OH}$  at  $75^\circ\text{C}$ . As the fraction  $x$  of Ge was increased, higher selectivity was obtained due to the decrease of the etch rate of the  $\text{Si}_{1-x}\text{Ge}_x$ . The achievement of the excellent selectivity in a  $\text{Si}/\text{Si}_{1-x}\text{Ge}_x/\text{Si}$  heterostructure was clearly demonstrated by scanning electron microscopy. Surfaces of etched  $\text{Si}_{1-x}\text{Ge}_x$  samples were analyzed using x-ray photoelectron spectroscopy. The high etch selectivity obtained in  $\text{NH}_4\text{OH}$  is essentially due to a passivation-film effect at the  $\text{Si}_{1-x}\text{Ge}_x$  surface.

### Introduction

Selective chemical etching of Si or  $\text{Si}_{1-x}\text{Ge}_x$  has become a key technique in the fabrication of  $\text{Si}_{1-x}\text{Ge}_x/\text{Si}$  heterojunction devices<sup>1,4</sup> and new kinds of structures.<sup>5,7</sup> In the fabrication process of the heterojunction device employing thin Si or  $\text{Si}_{1-x}\text{Ge}_x$  layers, for example, it is often necessary to contact to buried Si or  $\text{Si}_{1-x}\text{Ge}_x$  layers. To make contact to buried  $\text{Si}_{1-x}\text{Ge}_x$  layers one needs to etch Si and vice versa. Thin film bond and etchback silicon on insulator (BESOI) of good quality was fabricated using a strained  $\text{Si}_{0.7}\text{Ge}_{0.3}$  as an etch-stop layer. An important process of the fabrication was to selectively etch Si over the  $\text{Si}_{0.7}\text{Ge}_{0.3}$ .<sup>5</sup> Recently, we proposed and successfully fabricated Si quantum wires based on selectively removing  $\text{Si}_{1-x}\text{Ge}_x$  from a  $\text{Si}/\text{Si}_{1-x}\text{Ge}_x$  trench array.<sup>7</sup>

During the last several years, therefore, the characteristics of several chemical wet etchants for selectively etching  $\text{Si}_{1-x}\text{Ge}_x$

and/or Si on  $\text{Si}_{1-x}\text{Ge}_x/\text{Si}$  heterostructures have been investigated.<sup>5,11</sup> Among them, two aqueous etchants to selectively etch Si over  $\text{Si}_{1-x}\text{Ge}_x$  were reported. One is the etchant composed of  $\text{KOH}:\text{K}_2\text{Cr}_2\text{O}_7:\text{propanol}:\text{H}_2\text{O}$ .<sup>6,10</sup> A selectivity of 40:1 was obtained recently in etching Si over B-doped  $\text{Si}_{0.7}\text{Ge}_{0.3}$ , but it is completely isotropic and requires the use of a hard mask.<sup>10</sup> Another is the mixture of ethylenediamines, pyrocatechol, and water (EPW), which was reported to etch Si over  $\text{Si}/\text{Si}_{1-x}\text{Ge}_x$  ( $x > 0.2$ ) with a high selectivity.<sup>11</sup> For a practical application, however, a selective chemical etching should be compatible with silicon integrated circuit (IC) processes. As a result, IC-compatible, nontoxic, anisotropic, simple, and highly selective etchants become important for processing high performance devices. Solutions based on ammonium hydroxide-water mixtures have been widely used in Si IC processes.<sup>12</sup> Koyama *et al.* investigated the etch characteristics of  $\text{Si}_{1-x}\text{Ge}_x$  alloy in an ammoniac wet cleaning solution  $\text{NH}_4\text{OH}:\text{H}_2\text{O}_2:\text{H}_2\text{O}$ .<sup>13</sup> It was observed that the etch rate of  $\text{Si}_{1-x}\text{Ge}_x$  was in the order of

\* Electrochemical Society Student Member.